REGIONAL SEISMIC THRESHOLD MONIORING

T. Kværna, E. Hicks, J. Schweitzer, and F. Ringdal

NORSAR

Sponsored by Defense Threat Reduction Agency

Contract No. DTRA01-00-C-0107

ABSTRACT

A database comprising a total of 45 events, selected to provide the best possible ray path coverage of the Barents Sea and adjacent areas, was compiled and reanalyzed in a consistent manner. This resulted in new regional attenuation relations for Pn and Sn, together with a preferred average velocity model to be used for predicting the travel times of regional phases. We have now applied these attenuation relations to investigate a regional threshold monitoring scheme for the Barents Sea area.

A grid system with an approximately 100-km grid spacing was deployed for the Barents Sea region, and the observations at the arrays, ARCES, SPITS, FINES and NORES, were then used for calculating threshold magnitudes for each of the grid points. During an interval without seismic signals, the threshold magnitudes showed large variations over the region, and, in particular, in the vicinity of each array. However, for the region around the island of Novaya Zemlya, the variations are modest, varying around a mean of magnitude 2.1-2.2.

In order to investigate in more detail the variations in threshold magnitudes for the Novaya Zemlya region, we deployed a dense grid with an areal extent of about 500 x 500 km around the former Novaya Zemlya nuclear test site. For each of the grid nodes, we calculated magnitude thresholds for the two-hour time interval 00:00 - 02:00 on 23 February 2002. At 01:21:12.1 there was an event with a magnitude of about 3, located about 100 km northeast of the former nuclear test site.

Regions of different sizes were constructed by selecting grid points within different radii from the former nuclear test site. Average, minimum and maximum threshold magnitudes were calculated for circular regions with radii of 20, 50, 100 and 200 km, respectively.

The most important result is that even for a target region with radius as large as 100 km, the variations in threshold magnitudes are all within 0.2 magnitude units. This applies both for the time interval with the event and for background noise conditions. For the investigated station geometry, it will therefore be meaningful to represent the monitoring threshold of the entire Novaya Zemlya region with the values of a single target point, together with the *á priori* determined uncertainty bounds.

We can therefore conclude that the experimental site-specific threshold monitoring which has been run daily by NORSAR for the past 5 years, aiming at the Novaya Zemlya test site, can be used with only minor adjustments to assess the threshold within 100 km of the site. This monitoring has shown that between 16 August 1997 and 23 February 2002, the threshold level has been consistently below 2.5, except during “interfering” large regional or teleseismic events located well outside the target region.

For areas with larger variations in threshold magnitudes, like in the vicinity of the arrays, a 100-km radius target region will obviously show larger differences between the maximum and minimum values. Examples illustrating this point will be shown.

OBJECTIVE

The main objective of this research is to develop and test a new, advanced method for applying regional seismic array technology to the field of nuclear-test-ban monitoring. To that end, we address the development and testing of a method for optimized seismic monitoring of an extended geographical region, using a sparse network of regional arrays and three-component stations. Our earlier work on optimized site-specific threshold monitoring serves as a basis for the development of this new method. Emphasis of the research is on algorithms that can be efficiently applied in a real-time monitoring environment, that are using primarily automated processing, and that can be readily implemented in an operational Comprehensive Nuclear-Test-Ban Treaty (CTBT) monitoring system.

RESEARCH ACCOMPLISHED

Travel times and attenuation relations for regional phases in the Barents Sea region

A database containing 45 events in the Barents Sea region (Figure 1) has been compiled and analyzed with the aim of evaluating crustal models, travel times, and attenuation relations in the context of performing regional detection threshold monitoring of this region. The 45 events are mostly located around the circumference of the study area due to the virtually aseismic nature of the Barents Sea itself. Regional Pn and Sn phases were observable for most events in the database, while Pg and Lg phases were only observable for events with ray paths that do not cross the tectonic structures in the Barents Sea. This corroborates a number of previous observations of Lg-wave blockage within the Barents Sea.

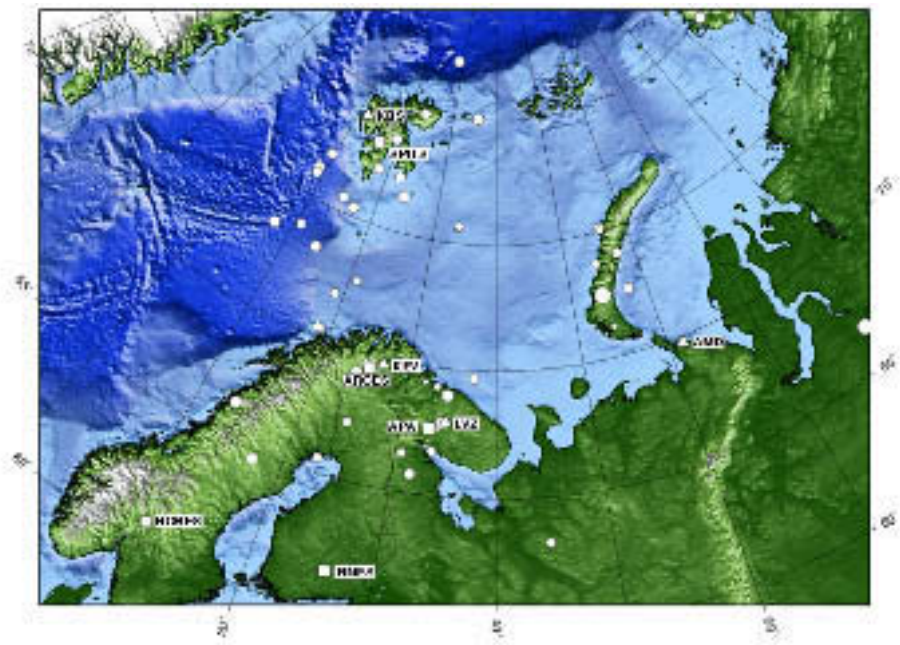

Figure 1. EVENTS (circles) and seismic stations used for deriving wave propagations characteristics of the Barents Sea and surrounding areas. Array stations are shown as squares, while three-component stations are shown as triangles. The symbol sizes for the events are proportional to the network magnitudes.

In order to estimate magnitudes, short-term average (STA) and spectral amplitude values were calculated in several frequency bands for all phase arrivals in the data base. There were no significant differences between spectral and STA amplitudes, so the latter were used since this parameter is more efficient to calculate in real-time processing. A joint inversion of the regional phases Pn, Pg, Sn and Lg was performed in order to determine attenuation relations specific for this region according to the relation given in Equation 1.

$$\mathbf{M_L} = \log \mathbf{A} - \log \mathbf{e} \cdot \alpha_{\mathbf{i}}^{0} \cdot \mathbf{f} + (\mathbf{a_i f} + \mathbf{b_i}) \log\left(\frac{200}{\Delta}\right) + \delta_{\mathbf{ik}} + 1.66 \qquad (1)$$

where A is observed STA amplitude within a frequency band with logarithmic center frequency f, Δ is epicentral distance, the α^0_i term represents the total attenuation for phase i out to the reference distance of 200 km, and a_i and b_i are phase-dependent attenuation constants. The inversion results for the parameters α^0, a and b are given in Table 1.

Table 1. The inversion results for the a, b and a0 coefficients (±1s) for Pn, Sn, Pg and Lg phases used in the attenuation relation (Equation 1).

Phase	a	b	α
P_n	-0.002 ± 0.023	2.340 ± 0.099	0.584 ± 0.030
S_n	0.141 ± 0.028	2.021 ± 0.110	0.419 ± 0.037
P_g	0.091 ± 0.084	0.851 ± 0.366	-0.538 ± 0.035
L_g	0.534 ± 0.062	-0.186 ± 0.123	-0.609 ± 0.063

Figure 2 shows a comparison between the phase magnitude residuals calculated using the relations and parameters of Jenkins *et al*. (1998) and our inversion results. Our results using the relations and parameters of Jenkins *et al*. (1998) revealed a relatively high scatter between individual station and phase magnitudes, and also some systematic inconsistencies, most notably magnitudes calculated from different frequency bands at the same station. Magnitudes calculated from STA values in the 2- to 4-Hz passband are mostly higher than magnitudes calculated in the 3- to 6-Hz passband, which again are generally higher than magnitudes calculated from the 4- to 8-Hz passband. The coefficients used in this case were determined using data from eastern North America, central Asia, and Australia. However, this relation is not primarily intended for local magnitude calculation, and some of the scatter in the magnitudes from Pg and Lg arrivals in particular may be due to the small distance for some of these observations, below the lower distance limit of 1.8° used by Jenkins *et al.* (1998).

Phase magnitudes calculated using Equation 1 and the parameters of Table 1 are shown to the right of Figure 2. These results show that the scatter (expressed as standard deviation) was significantly reduced compared to the original calculations. There is also no apparent frequency dependency in the magnitude residuals.

As an example we show in Table 2 the individual phase magnitude estimates of the 23 February 2002 event located on the northeastern coast of Novaya Zemlya. The consistency of these phase magnitudes is remarkably high.

Table 2. Phase magnitudes and network magnitudes for the 23 February 2002 event located on the northeastern coast of Novaya Zemlya, using the attenuation relations developed in this study.

Station	Phase	Distance	Magnitude
AMD	Pn	509	3.19
AMD	Sn	509	3.15
LVZ	Pn	1055	3.22
LVZ	Sn	1055	3.01
SPITS	Pn	1095	3.44
SPITS	Sn	1095	3.11
ARCES	Pn	1144	2.97
ARCES	Sn	1144	3.08
KBS	Pn	1197	3.16
KBS	Sn	1197	3.19
FINES	Pn	1850	3.17

Magnitude Type	Magnitude
Network Pn	3.19
Network Sn	3.11
Network All	3.15

Figure 3 shows comparisons of corrected network magnitudes compared to magnitudes calculated from individual phases. Although relative P and S magnitudes could be used as an aid in discriminating earthquakes and explosions, Figure 3 shows that regional path effects in this area also give rise to substantial differences in magnitude. This is particularly visible for Pn and Sn magnitudes, as they are available for events covering the entire region. Events that predominantly have ray paths within Fennoscandia have larger Sn magnitudes, while the opposite is true for events that have ray paths crossing the sediment basins of the Barents Sea (Novaya Zemlya/Kara Sea and the western Barents Sea/Mid-Atlantic ridge areas).

From this study, it is clear that Pn and Sn are the most useful phases for calculating magnitudes for events in the Barents Sea. In fact, Figure 3 shows that Pg and Lg are mainly observed at close epicentral distances (< 300 km). This situation is quite different from what we have previously found for the Scandinavian Peninsula and the Baltic Shield, where Lg is the dominant phase on the seismogram out to at least 1000 km. Thus, even for a stable continental region, one may expect quite significant regional variations in the magnitude correction factors.

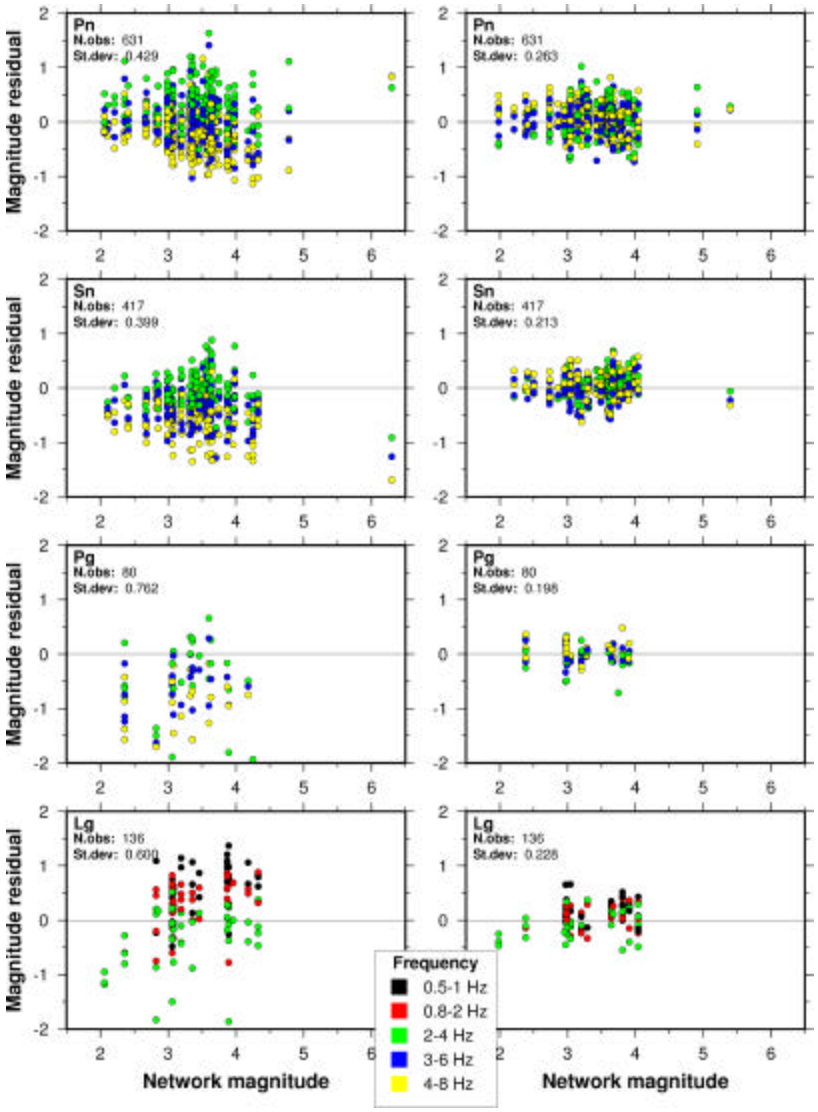

Figure 2. Magnitudes calculated using the relation from Jenkins *et al*. (1998) (left) and this study (right) from individual amplitude readings, plotted vs. network magnitudes for the 45 events. Note the significant reduction in scatter (St. Dev.) and also the absence of frequency-dependent effects when the relation from this study is used.

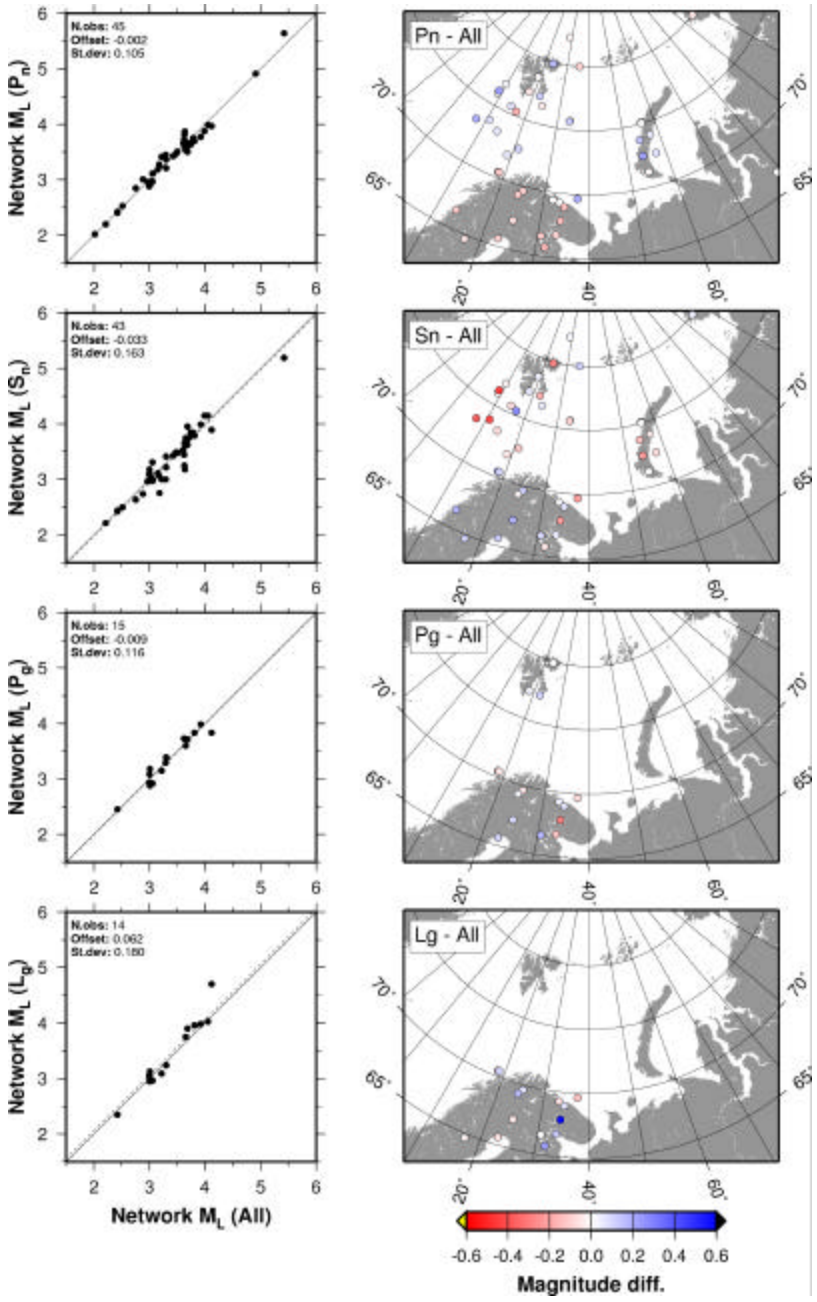

Figure 3. Network event magnitude comparisons and maps of the geographical distribution of the magnitude differences for individual phase magnitudes compared to network magnitudes. Note that Sn magnitudes are overestimated for events that have paths predominantly within the Baltic Shield, while events with paths that cross the Barents Sea have lower Sn magnitudes. Pg and Lg magnitudes appear to be quite stable within the limited distance range from which readings are available.

Regional Threshold Magnitudes

Using the developed attenuation relations described above, observations at the arrays ARCES, SPITS, FINES and NORES were used for calculating threshold magnitudes for a grid system covering the entire Barents Sea region. The grid spacing was approximately 100 km. Figure 4 shows the threshold magnitudes during a time instant without seismic signals. We find large variations over the region, and in particular when approaching each of the arrays. However, for the region around the island of Novaya Zemlya (NZ) the variations are modest, varying around a mean of magnitude 2.2.

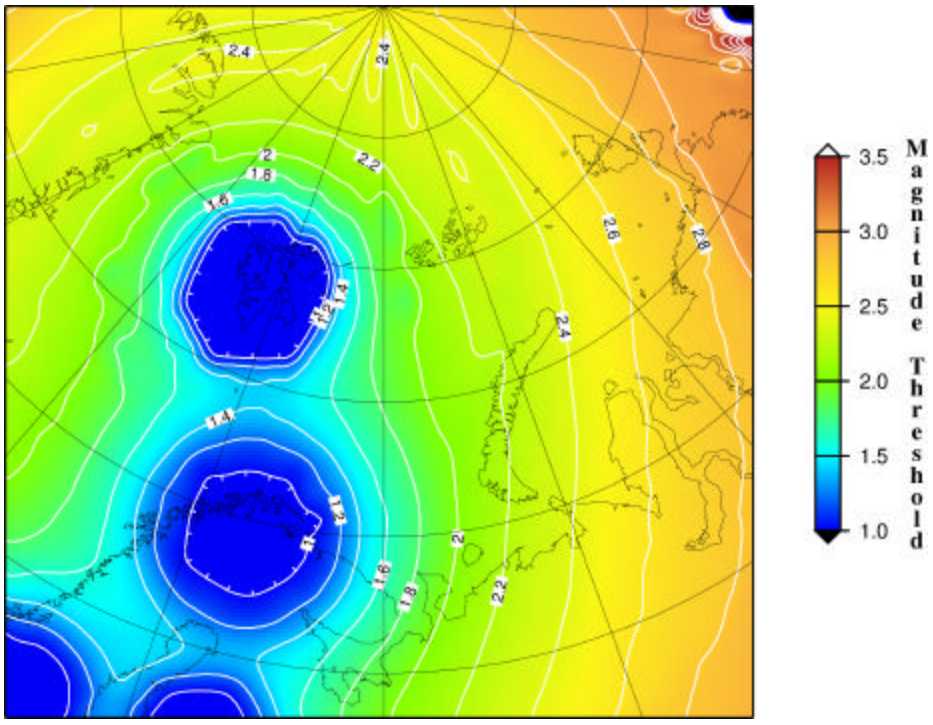

Figure 4. Threshold magnitudes for the time instant 2002-054:01.11.20.0. Notice the improved monitoring capability in the vicinity of each station. For distances above 1.5 degrees of each station, we have considered the Pn and Sn phases, whereas Pg and Lg have been used for distances less than 1.5 degrees.

In order to investigate in more detail the variations in threshold magnitudes for the Novaya Zemlya region, we deployed a dense grid with an areal extent of about 500 x 500 km as shown in Figure 5. For each of the grid nodes, we calculated magnitude thresholds for the two-hour time interval 00:00 - 02:00 on 23 February 2002. At 01:21:12.1 there was an event with a magnitude of about 3.2 (see Table 2), located about 100 km northeast of the former nuclear test site.

Regions of different sizes were constructed by selecting grid points within different radii from the former nuclear test site. Figure 6 (left) shows the variations in threshold magnitudes for a circular region with a radius of 20 km around the test site. The blue line shows the average threshold, whereas the red lines represent the minimum and maximum values. Figure 6 (right) shows similar curves for a region with radius 100 km.

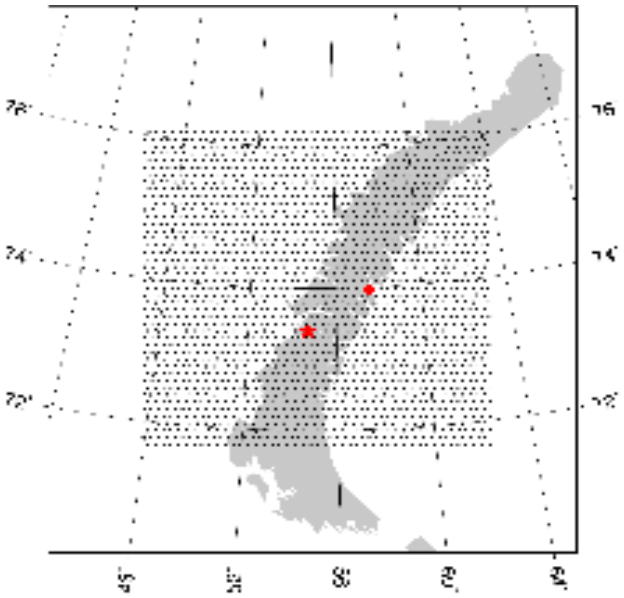

Figure 5. Dense grid deployment around Novaya **Z**emlya (grid spacing 11 km). The red star shows the location of the former nuclear test site, whereas the red diamond shows the location of the event on 23 February 2002 with origin time 01:21:12.1.

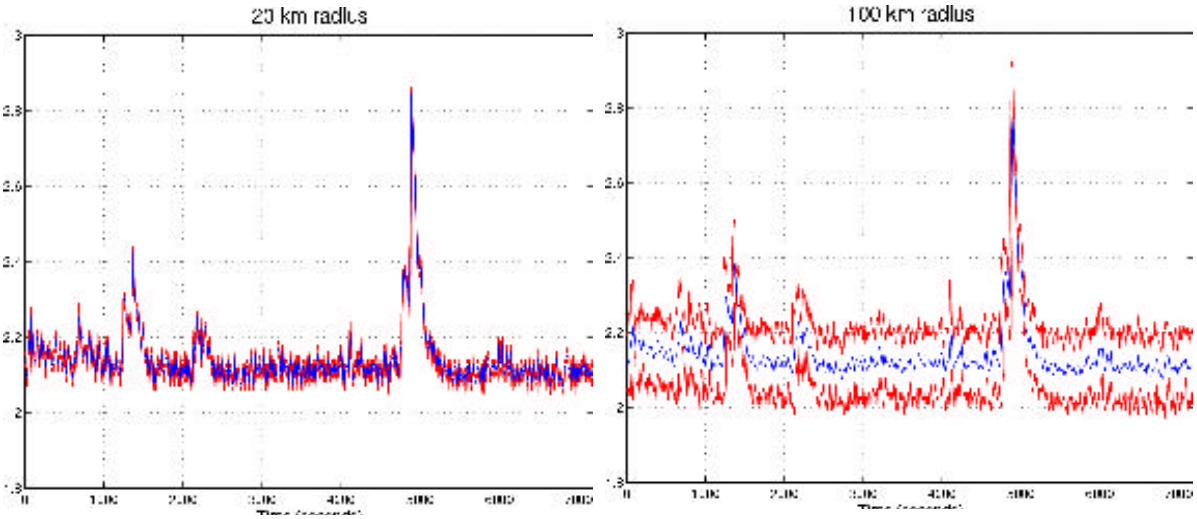

Figure 6. Threshold magnitudes for the time interval 00:00 - 02:00 on 23 February 2002 for 20-km (left) and 100-km (right) radius target regions centered around the former nuclear test site. The peak at about 5000 seconds corresponds to signals for the 3.2 event located about 100 km northeast of the test site.The blue line shows the average threshold, whereas the red lines represent the minimum and maximum values.

It is interesting to notice that even for a region with 100-km radius, the variations in threshold magnitudes are all within 0.2 magnitude units. For this particular configuration of the monitoring network relative to the target area, it will therefore be meaningful to represent the monitoring threshold of the entire region with the values of a single target point, together with uncertainty bounds as shown in Figure 6. For areas with larger variations in threshold magnitudes, like in the vicinity of the arrays, a 100-km radius target region will obviously show larger differences between the maximum and minimum values.

We would like to comment on the threshold magnitude of the peak corresponding to the event located northeast of the test site. In cases where an event actually occurs in the target region, the magnitude thresholds will often be biased slightly low. In Figure 6 we find a maximum value of about 2.9, whereas the event magnitude is estimated to be 3.15. In such cases a maximum-likelihood magnitude estimation algorithm should be activated. However, for small events with a size close to the threshold magnitudes, this bias will not be significant.

Regional threshold monitoring including the Amderma Station

The Kola Regional Seismic Center (KRSC) group in Apatity, Russia, has provided us with about three days of continuous data from the station in Amderma, located on mainland Russia, just south of the island of Novaya Zemlya. The data interval is centered around the origin time of the 23 February 2002 event located on the northeastern coast of Novaya Zemlya. In addition, data from the array in Apatity on the Kola Peninsula were included.

Figure 7 shows the threshold magnitudes during an instant without seismic signals, using the developed attenuation relations for Pn, Pg, Sn and Lg. We find large variations over the region, and in particular when approaching each of the arrays. With the Amderma Station included, we also find significant variations for the island of Novaya Zemlya, ranging from 1.4 at the southern tip to 2.2 at the northern tip. This implies that a regional threshold monitoring scheme for the NZ region has to be divided into geographical sub-regions having similar threshold magnitudes during background noise conditions.

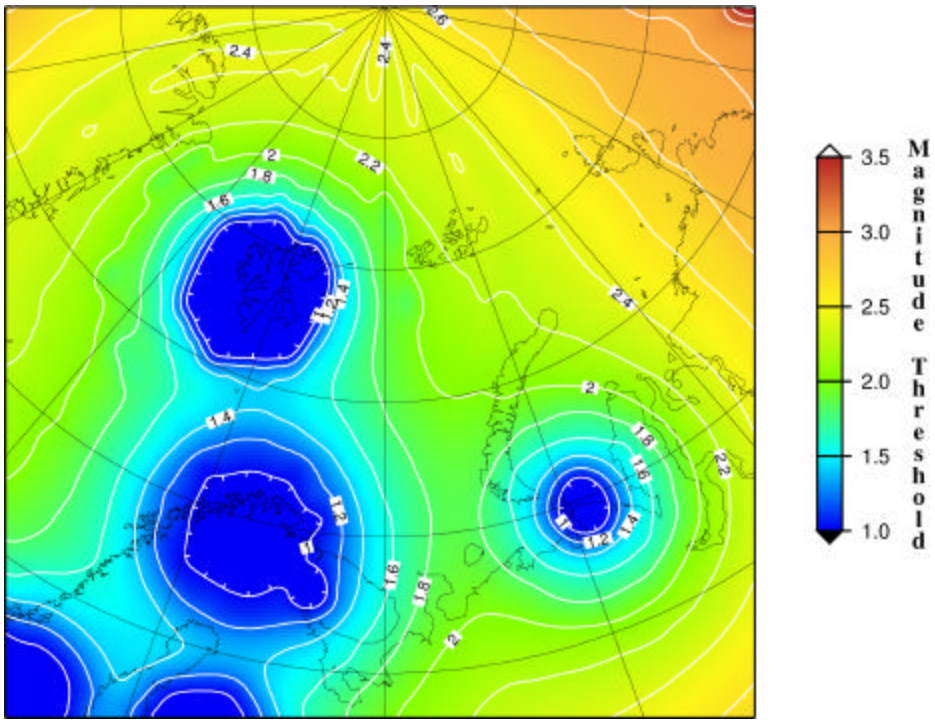

Figure 7. Threshold magnitudes for the time instant 2002-054:01.11.20.0, including data from the Amderma Station and the Apatity Array. Notice the improved monitoring capability in the vicinity of the Amderma Station as compared to the thresholds shown in Figure 4.

CONCLUSIONS AND RECOMMENDATIONS

The pattern of Lg arrivals and associated amplitudes supports the previously published indications that the deep sediment basins and Moho topography under the Barents Sea efficiently block Lg wave energy from crossing. From this, it is clear that Pn and Sn are the most useful phases for calculating stable and consistent magnitudes for events in the Barents Sea.

The 'BAREY' model from Schweitzer and Kennett (2002), based on a model for the Barents Sea area from Kremenetskaya *et al*. (2001), provides the smallest overall travel-time residuals when locating events within the vicinity of the Barents and Kara Seas.

The attenuation in the Barents Sea region differs somewhat from that observed in other stable tectonic regions, as evidenced by the fact that the coefficients given by Jenkins *et al.* (1998) for such regions do not give consistent magnitudes across frequencies, phases and stations for our amplitude observations from the events in the Barents Sea region.

Amplitude inversion has been used in this study to resolve new attenuation coefficients and station corrections for estimating magnitudes from STA amplitude observations for Pn, Pg, Sn and Lg phases in the Barents Sea region. The distance range of observations on which the Pg and Lg relations are based is limited; a future study using a greater number of continental events could most likely provide a relation for STA-based Lg magnitudes that is applicable at larger distances, albeit limited to paths within Fennoscandia.

The seismic station in Amderma can be tied in to the regional network in Fennoscandia and on the Svalbard Archipelago using an appropriate crustal model, and is able to provide important information regarding the location of events in the eastern parts of the Barents Sea and the Kara Sea (Schweitzer and Kennett, 2002). Magnitudes calculated at this station are, on the whole consistent, with the other observations.

For the time interval under study, the seismic arrays ARCES, SPITS, FINES and NORES provide an average monitoring capability of about magnitude 2.2 for the island of Novaya Zemlya. For a region with a 100-km radius around the former nuclear test site, the variations in threshold magnitudes are all within 0.2 magnitude units. It will therefore be meaningful to represent the monitoring threshold of the entire region with the values of a single target point, together with uncertainty bounds as shown in Figure 6.

In cases when data from the Amderma Station can be retrieved, we find significant variations in threshold magnitudes over the island of Novaya Zemlya, ranging from 1.4 at the southern tip to 2.2 at the northern tip. For the actual time interval, the monitoring capability for the former nuclear test site is lowered by about 0.3 magnitude units to about 1.9. This implies that a regional threshold monitoring scheme for the NZ region has to be divided into geographical sub-regions having similar threshold magnitudes during background noise conditions.

REFERENCES

Jenkins, R.D., T.J. Sereno, and D.A. Brumbaugh (1998), Regional attenuation at PIDC stations and the transportability of the S/P discriminant. AFRL-VS-HA-TR-98-0046, Science Applications International Corporation, San Diego, CA, USA.

Kremenetskaya, E., V. Asming, and F. Ringdal (2001). Seismic location calibration of the European Arctic, *Pure Appl. Geophys.* **158**, 117-128.

Schweitzer, J. and B.L.N. Kennett (2002), Comparison of location procedures - the Kara Sea event 16 August 1997, Semiannual Technical Summary, 1 July - 31 December 2001, NORSAR Sci. Rep. 2-2001/2002, Kjeller, Norway, 97-114.